Bionanoparticles as Candidate Reference Materials for Mobility Analysis of Nanoparticles

R. You,[§,‡] M. Li,[§,‡] S. Guha,[§,‡,†] G. W. Mulholland,[§,‡] and M. R. Zachariah*,[§,‡]

[§]University of Maryland, College Park, Maryland 20742, United States

[‡]National Institute of Standards and Technology, Gaithersburg, Maryland 20899, United States

ABSTRACT: We propose bionanoparticles as a candidate reference material for determining the mobility of nanoparticles over the range of $6 \times 10^{-8} - 5 \times 10^{-6}$ $m^2V^{-1}s^{-1}$. Using an electrospray differential mobility analyzer (ES-DMA), we measured the empirical distribution of several bionanoparticles. All of them show monomodal distributions that are more than two times narrower than the currently used calibration particles for mobility larger than 6×10^{-8} $m^2V^{-1}s^{-1}$ (diameters less than 60 nm). We also present a numerical method to calculate corrected distributions of bionanoparticles by separating the contribution of the diffusive transfer function. The corrected distribution is about 20% narrower than the empirical distributions. Even with the correction, the reduced width of the mobility distribution is about a factor of 2 larger than the diffusive transfer function. The additional broadening could result from the nonuniform conformation of bionanoparticles and from the presence of volatile impurities or solvent adducts. The mobilities of these investigated bionanoparticle are stable over a range of buffer concentration and molarity, with no evidence of temporal degradation over several weeks.
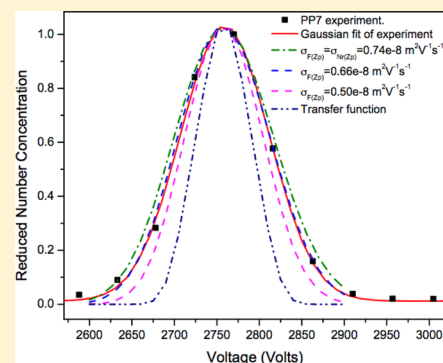
With the proliferation of nanoparticle based materials in applications as diverse as photonics to nanomedicine and the associated concerns about exposure and toxicology, reliable metrology characterization tools and materials necessary to calibrate them are needed.[1] One tool that has been rapidly increasing in general nanoparticle metrology is differential mobility analysis (DMA) and its variant electrospray differential mobility analysis (ES-DMA).[2] Characterization based on the DMA is a very powerful instrumental approach to measure the complete mobility/size distribution of nanoparticles in the gas phase. The method relies on a characterization of the electrical mobility Z_p of aerosolized nanoparticles (NPs) by balancing the electric and drag force on the particles. The relationship between particle diameter D_p and electrical mobility Z_p is shown in eq 1 with C_c being the slip correction factor and η being the viscosity of air. The DMA can be used to achieve size-selection of NPs by fixing the voltage between two electrodes or to obtain size-distribution by scanning the voltage.[3,4]

$$Z_p = \frac{neC_c(D_p)}{3\pi\eta D_p} \quad (1)$$

While this ion-mobility approach offers superior resolution and accuracy, this can only be realized by an absolute calibration, using a well calibrated source. Various noncertified reference materials (RMs) and standard reference materials (SRMs) for nanoparticle sizing are commercially available,[5] including polystyrene latex spheres (PSLs), metallic NPs (e.g., colloidal gold and silver NPs), and metal oxides (e.g., colloidal silica), in the form of particle suspensions, in which nonvolatile

additives, like citrate, are very often added to stabilize the particles in the solution. One difficulty in the production of these standards is that it is not possible to synthesize a new batch of particles with an identical size distribution as a previous batch. Thus, it is not possible to issue a replacement standard with the same particle mobility/size as a previous standard.

In contrast to "engineered" NPs as described above, biologically derived materials, referred to as bionanoparticles henceforth, offer a precision in reproduction that cannot be matched. The size and shape of each bionanoparticle is highly repeatable. This can lead to an almost perfectly monodispersed aerosol while the "engineered" nanospheres have relatively broad distributions for sizes of 60 nm and less. Moreover, since commercially available bionanoparticles are usually lyophilized (available as dry powders) to keep the samples stable, their suspensions can be made at as high concentrations as required.

Currently, a series of unique molecular ions (tetra-alkyl ammonium ions) is being used in the calibration of high flow DMA capable of measuring mobility over the range of $5 \times 10^{-6} - 100 \times 10^{-6}$ $m^2V^{-1}s^{-1}$ (diameter of 1 to 6 nm).[6,7] The widely used low flow nanoDMAs (TSI, Grimm etc.) are capable of measuring mobilities in the range of $0.06 \times 10^{-6} - 20 \times 10^{-6}$ $m^2V^{-1}s^{-1}$ (with diameters ranging from 3 to 60 nm). The bionanoparticles considered in this study cover the size range appropriate for the calibration of the low flow DMAs.

In this paper, we explore using biologically derived materials as potential particle mobility/size standards for the DMA. The first implementation of ES-DMA to bionanoparticles can be traced back to 1996, when Kaufman et al. measured globular proteins ranging from 3 to 14 nm.[8] Subsequently, researchers have presented the application of this technique to other specific bionanoparticles such as polymers, viruses, bacteriophages, etc.[9−12] Most of them, however, were investigated only at a modest resolution, and the actual width of the mobility size distributions remained unknown. One recent study by A. Maiβer using high flow DMA included bovine serum albumin (BSA), which is included in our study, to provide an overlap between the high flow and low flow DMA measurements.[6] Here, we systematically investigated five different bionanoparticles: BSA, polyclonal human immunoglobulin (IgG), a glycoprotein with a high glyan heterogeneity, phage PP7, coliphage PR772, and tobacco mosaic virus (TMV) with size ranging from 6 nm up to 64 nm. The measurements of these materials were compared with high precision "engineered" nanoparticles: gold colloids (AuNPs) and polystyrene latex beads (PSL). We also calculated corresponding transfer functions and separated its contribution from the measured distribution in order to further estimate the true width of the size spectrum for each aerosolized bionanoparticle. To demonstrate the stability of these bionanoparticles, the mobility/size was measured for a range of bionanoparticle suspension concentration and buffer molarity. Day-to-day variation of mobility/size was also evaluated. We conclude from these results that bioderived material offer superior calibration of mobility-analysis equipment over most "engineered" nanoparticles. It is worth noting that size measured by DMA could differ from device to device up to 15% even for the same analyte.[13] Hence, the model of the equipment should be specified, and a round robin test is important before assigning the value for reference material, which is beyond the scope of the discussion in this paper.

■ EXPERIMENTAL SECTION

Electrospray Particle Generation and Differential Mobility Measurements. We measured the size distribution with an ES-neutralizer-DMA-condensation particle counter (ES-neutralizer-DMA-CPC) system described previously.[14] Suspended bionanoparticles were first aerosolized using a 40 μm inner diameter capillary mounted in an electrospray (TSI Inc., Shore View, MN, #3480) with the chamber pressure of 2.55×10^4 Pa (3.7 psi) and a carrier gas of 20 cm^3/s (1.2 L/min) purified air. The aerosolized droplets were then charge-reduced in a Po-210 radiation source so that most aerosols carry −1, 0, or +1 charge. A negative voltage was applied to the central electrode of a Nano DMA (TSI Inc., #3085) such that the +1 charged particles passed through the DMA and were counted by a condensation particle counter (CPC) (TSI Inc. #3025A), counting efficiency of which is over 95% for the investigated sizes. Two modules of mass flow controller (MKS Inc., #M100B), 333.3 cm^3/s (20 000 sccm) and 500 cm^3/s (30 000 sccm), were used to control the sheath flow in the DMA, accuracy of which is ±5 cm^3/s (300 sccm) and ±10 cm^3/s (600 sccm), respectively.

The investigated bionanoparticles were split into two groups based on their expected mobility size. For smaller particles, i.e., IgG, BSA, and PP7, a high sheath flow rate of 500 cm^3/s (30 L/min) was adopted to reduce the broadening of the DMA transfer function from Brownian motion. For the larger

particles, i.e., PR772 and TMV, a sheath flow rate of 83.33 cm^3/s (5 L/min) was used so that the largest particle could be sampled at a voltage below the maximum value of 10 000 V for the power supply. Due to anticipated narrow size distributions of bionanoparticles, the ratios of the sheath to aerosol flow were chosen to be large, about 42 for smaller particles and 33 for the larger ones. Since the resolution in a DMA scales as the ratio of the sheath to aerosol, the operating resolution of the DMA is higher than what is normal practice. To ensure this resolution, the DMA was operated in a voltage stepping mode with an interval of 25 s at high sheath flow and 40 s under low flow rate, which ensured that the residence time from DMA inlet to the CPC detector was smaller than the dwell time. The scanning interval is chosen to be 0.2 nm for the smaller bionanoparticles, particularly 0.05 nm for BSA, and 1 nm for the larger ones. For the purpose of equipment calibration, NIST SRM PSL of 100.7 nm, SRM1963, was used in the measurements of big bionanoparticles while 30 nm citrate-stabilized AuNPs (Ted Pella Inc.), size-calibrated by SRM 1963, were employed in those of small biomolecules. For the size distribution measurement of citrate-stabilized AuNPs, we refer the readers to Hinterwirth's paper[15] which gives comparative assessment of several characterization methods and shows that ES-DMA has the highest size resolution.

The voltage associated with centroid electrical mobility was assigned by averaging the means of Gaussian fits to three replicate measurements. Electrical mobility of each bionanoparticle was calculated as below.

$$Z_p = \frac{Q_{sh} \ln \frac{r_{out}}{r_{in}}}{2\pi V_e L_d} \tag{2}$$

where Q_{sh} is the sheath flow rate, r_{out} and r_{in} are the outer and inner radii of DMA column, V_e is the voltage applied on electrodes, and L_d is the length of DMA column. The mobility size in this paper was calculated using eq 1, in which the slip correction factor is given by

$$C_c(D_p) = 1 + K_n[A_1 + A_2 \exp(-A_3/K_n)] \tag{3}$$

where K_n is twice the mean free path of air divided by the particle diameter ($K_n = 2\lambda/D_p$) and $A_1 = 1.142$, $A_2 = 0.558$, and $A_3 = 0.999$.[16] Eq 3 is an empirical and alternative expression[11] that has been suggested for describing the relationship between mobility and particle diameter for small particles in the size range of less than 10 nm. The fundamental quantity accurately measured by the DMA is the mobility of the particle, while the determination of the mobility diameter has additional uncertainty from the use of eq 3. We present our results in terms of mobility diameter as well as mobility because of the widespread use of mobility diameter in the aerosol community.

ES-DMA Buffer Preparation. Twenty mM ammonium acetate buffer solutions (AmAc) were prepared by dissolving 0.77 g of ammonium acetate powder (Sigma-Aldrich, St. Louis, MO, #631-61-8) in 0.5 L of deionized water (18 MΩ/cm, Barnestead nanopure UV system) filtered by 0.2 μm pores. Ten and two mM buffers were then obtained by diluting with filtered deionized water.

Bionanoparticle Suspension Preparation. We found that to obtain well-shaped mobility spectra with minimal capillary clogging of the electrospray the optimized sample concentration should yield a CPC count ranging from 2000 to 6000 particles/cm^3. The easiest approach to achieve this target was to start with highly concentrated solutions and dilute with
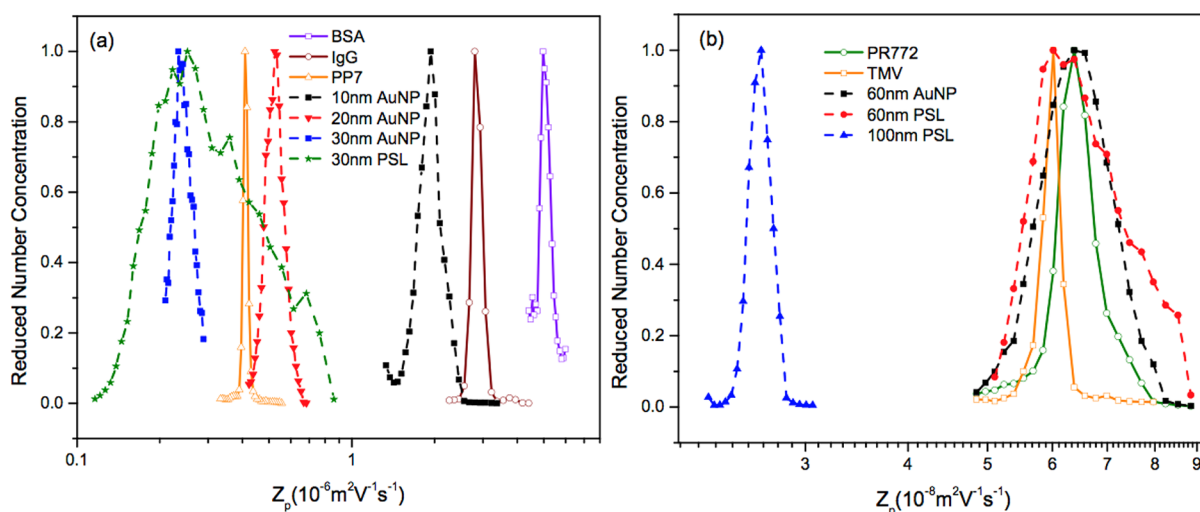
Figure 1. Comparison of mobility distribution between smaller bionanoparticles (a) and bigger bionanoparticles (b) with engineered nanoparticles with comparable size.

Table 1. Standard Deviation of Distribution of Bionanoparticles and "Engineered" NPs

	Z_p (10^{-8} m^{2}V^{-1}s^{-1})	$\sigma_{Z_p,exp}$ (10^{-8} m^{2}V^{-1}s^{-1})	$\sigma_{r,Z_p,exp}$	D_p (nm)	$\sigma_{D_p,exp}$ (nm)	$\sigma_{r,Z_p,exp}$
		Bioparticles				
BSA	465.9	21.8	0.047	6.80	0.16	0.023
IgG	261.2	11.2	0.043	9.11	0.20	0.022
PP7	36.99	0.736	0.020	24.58	0.22	0.009
PR772	6.41	0.292	0.046	61.64	1.42	0.023
TMV	6.09	0.127	0.021	63.38	0.70	0.011
		"Engineered" NP				
AuNP 10 nm	193.2	12.2	0.063	10.6	0.343	0.032
AuNP 20 nm	52.48	3.96	0.075	20.6	0.824	0.040
AuNP 30 nm	24.01	1.03	0.043	30.8	0.714	0.023
PSL 30 nm	25.74	4.57	0.178	30.26	3.754	0.123
AuNP 60 nm	6.439	0.611	0.095	62.0	3.319	0.054
PSL 60 nm	6.255	0.479	0.077	62.8	3.003	0.048
PSL 100.7 nm	2.641	0.088	0.033	101	1.769	0.018

buffer. For BSA (Sigma-Aldrich, St. Louis, MO, # A9418), and human IgG (Sigma-Aldrich, St. Louis, MO, # 14506), initial solution was prepared by suspending 1 mg in 1 mL of 20 mM AmAc. The solution was then diluted to be 100 μg/mL and denoted as a 1× dilution. Phage PP7 from ATCC (Manassas, VA; accession numbers 15692-B4) and PR772 (Felix d'Herelle Reference Center for Bacterial Viruses, Universite Laval, Quebec, Canada) were prepared as described in a previous paper.[17] The initial solutions were obtained with a concentration of 2.5 × 10^{13} plaque forming units/cm^3 (pfu/cm^3) and 1.5 × 10^{12} pfu/cm^3, respectively. The phages were then dialyzed into 20 mM AmAc and adjusted to 2.1 × 10^{11} pfu/cm^3 for PP7 and 1.25 × 10^{10} pfu/cm^3 for PR772 in a 1× dilution. A TMV suspension (James N. Culver's Lab, UMD) with an initial concentration of 15 mg/mL was diluted to 50 μg/mL with 2 mM AmAc for 1× dilutions. Samples with five (5×) and ten (10×) times dilutions were also made to assess the effect of concentration on the mobility size. To assess the stability of bionanoparticle size in buffers with different molarities, 10 and 2 mM AmAc were used to prepare 5× solutions for IgG and BSA as well as 1× solutions for PP7 and PR772. For TMV, 1× solutions were also prepared using 10 and 20 mM buffers.

"Engineered" NPs Suspension Preparation. Size distributions of "engineered" NPs including 10, 20, 30, and

60 nm citrate-stabilized monodispersed colloidal AuNPs (Ted Pella Inc.) were measured. A suspension (1.5 mL) of 10 nm AuNPs were first centrifuged at 13.2 kRPM for 40 min to remove most of the supernatant and then replaced with an equivalent volume of 2 mM AmAc. This process was repeated to remove the citrate stabilizer, which forms a residue on the surface of the gold particle if not removed. The same procedure was applied to 20, 30, and 60 nm AuNPs by changing the centrifuge time to 15, 3, and 1 min, respectively. For the PSL spheres, a drop of SRM 1963 was mixed with 1 mL of 2 mM AmAc and diluted 6 times. The same procedure was applied to 30 nm PSLs (Thermo Scientific. 3030A) and 60 nm PSLs (NIST SRM1964) with a dilution factor of 20 for the 30 nm sample and 10 for the 60 nm sample.

■ RESULTS AND DISCUSSION

Homogeneity of Bionanoparticle. *Comparison of Measured Distribution with Engineered Particles.* Figure 1 shows a typical plot of number concentration reduced by the peak value, $N_r(Z_p)$, versus mobility for bionanoparticles and comparison to AuNPs and PSLs spheres. The standard deviations of the mobility distribution $\sigma_{Z_p,exp}$ and of the size

6838

dx.doi.org/10.1021/ac403503q | *Anal. Chem.* 2014, 86, 6836–6842
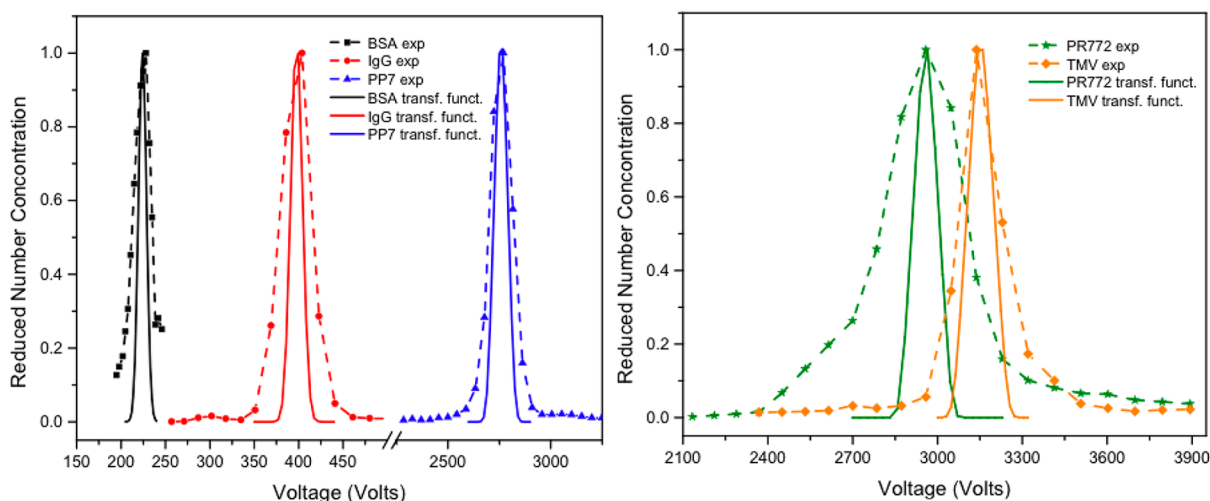
Figure 2. Comparison of experimental size distribution with the corresponding diffusive transfer function normalized to the maximum value.

Table 2. Standard Deviation of the Corrected Mobility Distribution and That of the Corresponding Size Distribution of Bionanoparticles[a]

	Z_p (10^{-8} m^{2}V^{-1}s^{-1})	$\sigma_{r,Z_p,exp}$	$\sigma_{r,Z_p,transf}$	$\sigma_{r,Z_p,F(Z_p)}$	D_p (nm)	$\sigma_{r,D_p,exp}$	$\sigma_{r,D_p,transf}$	$\sigma_{r,D_p,F(D_p)}$
BSA	465.9	0.047	0.020	0.041	6.80	0.023	0.011	0.015
IgG	261.2	0.043	0.017	0.037	9.11	0.019	0.008	0.012
PP7	36.99	0.020	0.012	0.016	24.58	0.009	0.006	0.008
PR772	6.41	0.046	0.016	0.042	61.64	0.025	0.008	0.023
TMV	6.09	0.021	0.014	0.017	63.38	0.012	0.008	0.009

[a]As for smaller bioparticles, i.e., BSA, IgG, and PP7, measurements were carried out with sheath flow of 30 L/min while the bigger ones, PR772 and TMV, were measured with sheath flow of 5 L/min.

distribution $\sigma_{D_p,exp}$ are listed in Table 1. The reduced standard deviations $\sigma_{r,Z_p,exp}$ and $\sigma_{r,D_p,exp}$ are calculated as

$$\sigma_{r,Z_p,exp} = \frac{\sigma_{Z_p,exp}}{Z_p}, \qquad \sigma_{r,D_p,exp} = \frac{\sigma_{D_p,exp}}{D_p} \tag{4}$$

In all cases, the bionanoparticles have narrower width of $N_r(Z_p)$ with reduced standard deviations that did not exceed 0.047. In contrast, among the engineered particles, only SRM 1963 (PSL 100.7 nm) has a comparable distribution with a $\sigma_{r,Z_p,exp}$ of 0.033. The colloidal gold samples are by far the better of the "engineered" particles relative to PSLs for sizes of 60 nm and lower in terms of monodispersity. It is also worth noting that the narrow distributions of bioparticles comprise both single molecules (e.g., IgG and BSA) as well as whole viruses (PP7, PR772, TMV). However, despite the remarkably narrow distribution of TMV ($\sigma_{r,Z_p,exp}$ = 0.021) and consistency of mobility measured over a long period of time as shown in the Stability of Bionanoparticle section, we suggest that it be used with an understanding of its length variation in solution and folded state after electrospray.[18]

Evaluation of Instrumental Resolution Limit. To assess if the observed size distributions reflect the intrinsic property of the particles or the resolution limit of the DMA, we evaluate the transfer function. The transfer function of the DMA is defined as the probability of an aerosol particle with a certain size that enters at the inlet slit and exits via the sampling slit.[3] As a good approximation, the transfer function including Brownian diffusion of the aerosol reflects the instrumental resolution limit. We calculated the transfer function according to Stolzenburg's approach[19] and found that the peak value of

the transfer function decreases, and the function broadens as particle mobility increases under the same experimental setup, as described in the literature.[20] For comparison with the experimental $N_r(Z_p)$, we normalize the DMA's diffusive transfer function to the peak value and compare them with corresponding $N_r(Z_p)$ of bionanoparticles in Figure 2. We also present the reduced standard deviations of the transfer function in mobility, $\sigma_{r,Z_p,transf}$, and that for mobility size, $\sigma_{r,D_p,transf}$, of all bionanoparticles in Table 2 for comparison. The distributions of the proteins, BSA and IgG, show standard deviations of $N_r(Z_p)$ that are about 2.4 times that of the respective transfer functions. The PP7 and TMV, which are both viruses, show standard deviations even closer to that of the transfer function. The PR772 virus showed a relatively wide distribution, 2.9 times larger than its transfer function. These results show that the bionanoparticles are monodispersed with the measured $N_r(Z_p)$ less than three times wider than the corresponding transfer function.

Calculation of Corrected Width of Bionanoparticle Distribution. As Knutson and Whitby's derivation[3] in 1975 shows, the number of particles, $N(V)$, measured at the outlet of the DMA at voltage V is the integral over the product of the DMA transfer function Ω and the mobility distribution $F(Z_p)$, as shown in eq 5 below

$$N(V) = \int_0^\infty \Omega(Z_p, V) F(Z_p)\, dZ_p \tag{5}$$

In most cases, the distribution of aerosols $F(Z_p)$ is broad relative to the transfer function $\Omega(Z_p, V)$. Hence, the standard approximation[3] is to treat $F(Z_p)$ as a constant value for the integration of the transfer function, in which case $F(Z_p)$ is

proportional to the empirical $N_r(Z_p)$ in Figure 1. However, this is clearly not the case for bionanoparticles. Due to their very narrow distribution, such an approximation could result in an overestimation of the true width of the distribution of bionanoparticles.

Here, we present a numerical method to evaluate the width of the bionanoparticle distribution $F(Z_p)$. Assuming $F(Z_p)$ to be Gaussian distributed with a standard deviation of $\sigma_{F(Z_p)}$, a spectral particle count as a function of voltage can be calculated using eq 5. This numerical result is compared with $N_r(Z_p)$, and the value of $\sigma_{F(Z_p)}$ that gives the best fit is considered as the width of the mobility distribution of the bionanoparticle. Figure 3 shows the numerical results of number spectra for PP7 as an
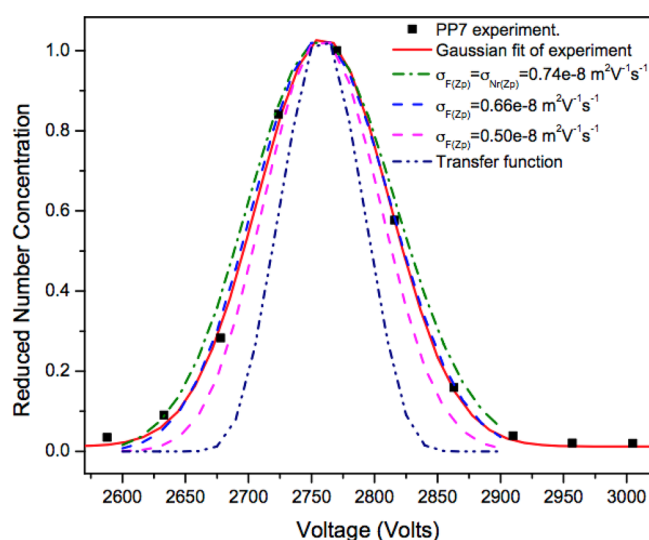
Figure 3. An example of numerical result of normalized number distribution as a function of voltage for PP7 with various widths. The best fit to the experimental data is for $\sigma_{F(Z_p)} = 0.66 \times 10^{-8}$ m²V⁻¹s⁻¹. The transfer function is also plotted for comparison.

example. The spectral distribution narrows as $\sigma_{F(Z_p)}$ decreases. The best fit spectral distribution to the experimental data is when $\sigma_{F(Z_p)}$ is 0.66×10^{-8} m²V⁻¹s⁻¹. The mobility distribution $F(Z_p)$ is further converted to a size distribution $G(D_p)$, according to

$$G(D_p) = \frac{F(Z_p)}{p(D_p)} \left| \frac{dZ_p}{dD_p} \right|$$

where $p(D_p)$ is the probability that a particle with diameter D_p carries one elementary unit of charge, and the reduced widths of distribution for bionanoparticles are listed in Table 2. The ratio of the reduced width of the corrected distribution to the

transfer function reduced width is in the range of 1.21 to 2.18 with an average value of 1.69 excluding the value for PR772.

Notice that the width of corrected distribution $F(Z_p)$ is not as small as expected: it is less than 20% smaller than the width of measured distribution; the distribution is proportional to the first order approximation of $F(Z_p)$, but it is still about two times bigger than that of the transfer function. This could also be explained by the possibility of differential residual water or impurities retained on bionanoparticles which leads to a broader distribution. Although nonvolatile impurities attachment was ruled out by A. Maiβer's study, possibilities of differential amounts of residual solvent or a volatile adduct cannot be eliminated, and they could attribute to the broad distributions.[6] A second possibility could be the conformation of bionanoparticles altered when being introduced to the gas phase.[6,21,22] Compaction of proteins and viruses was found after electrospraying.[6,18,23] Nonideal instrument performance of DMA could be another factor that attributes to the broad distribution (thereby reducing its resolving power). However, A. Maiβer et al. argued that the influence from instrumentation can be ruled out based on a similar observation as Kaufman's using different DMA.[6]

Stability of Bionanoparticle. When ammonium acetate buffer is used to dissolve bionanoparticle, ammonium cations could pair with acidic functional groups and acetate anion could pair with basic functional groups in the protein.[24] As a result, the concentration of ions in the buffer could be a potential factor that affects the size of the bionanoparticle. All results in Tables 3, 4, and 5 are shown with mobility and diameter of bionanoparticles as well as the standard deviation of the multiple measurements. Results in Table 3 suggest that the molar concentration of buffer has at most only a minimal effect on the resulting absolute mobility size. The effect of dilution, which should primarily affect the salt coating thickness on the particles after electrospray as seen in Table 4, shows a negligible effect.

Finally, we investigated long-term stability, which was assessed at 1 day, 1 week, and 4 weeks after. All samples were stored at 4 °C. As shown in Table 5, no significant day to day variation was observed in the mobility sizes, indicating that temporal degradation of the investigated bionanoparticles is negligible for at least up to 4 weeks. However, previous study of PR772 shows evidence of disintegration of the capsids after 11 weeks,[12] which indicates PR772 is not a good candidate reference material for a long-term use.

As a comparison of the mobility of BSA with prior studies, we notice our result is about 12% lower than the measurement from A. Maiβer et al. and, hence, results in a bigger inferred mobility size similar to what Kaddis et al. and Bacher et al. obtained. Also, we obtained a narrower distribution for BSA with fwhm (full width at half-maximum) of 11.0% compared to that of 17.6% from Maiβer. Though Maiβer et al. inferred that

Table 3. Mobility and Mobility Size of Bionanoparticles with Various Molarity of Ammonium Acetate

	20 mM AmAc		10 mM AmAc		2 mM AmAc	
	Z_p (10⁻⁸ m²V⁻¹s⁻¹)	D_p (nm)	Z_p (10⁻⁸ m²V⁻¹s⁻¹)	D_p (nm)	Z_p (10⁻⁸ m²V⁻¹s⁻¹)	D_p (nm)
BSA	464.19 ± 1.98	6.81 ± 0.02	457.48 ± 1.34	6.86 ± 0.01	436.07 ± 1.01	7.03 ± 0.01
IgG	260.65 ± 0.71	9.11 ± 0.01	260.52 ± 0.62	9.11 ± 0.01	251.18 ± 0.31	9.28 ± 0.01
PP7	36.99 ± 0.03	24.58 ± 0.01	37.18 ± 0.02	24.51 ± 0.01	36.75 ± 0.03	24.66 ± 0.01
PR772	6.42 ± 0.01	61.65 ± 0.01	6.44 ± 0.01	61.55 ± 0.02	6.40 ± 0.01	61.74 ± 0.05
TMV	6.10 ± 0.01	63.36 ± 0.03	6.10 ± 0.02	63.36 ± 0.11	6.11 ± 0.01	63.30 ± 0.06

Table 4. Mobility and Mobility Size as a Function of Dilution

	1×		5×		10×	
	Z_p (10^{-8} m^{2}V^{-1}s^{-1})	D_p (nm)	Z_p (10^{-8} m^{2}V^{-1}s^{-1})	D_p (nm)	Z_p (10^{-8} m^{2}V^{-1}s^{-1})	D_p (nm)
BSA	466.84 ± 0.97	6.79 ± 0.01	464.19 ± 1.98	6.81 ± 0.02	467.89 ± 2.03	6.86 ± 0.02
IgG	258.09 ± 0.89	9.15 ± 0.02	260.52 ± 0.62	9.11 ± 0.01	261.13 ± 0.40	9.10 ± 0.01
PP7	36.99 ± 0.03	24.58 ± 0.01	37.00 ± 0.06	24.57 ± 0.02	37.04 ± 0.03	24.56 ± 0.01
PR772	6.42 ± 0.01	61.65 ± 0.01	6.41 ± 0.01	61.66 ± 0.03	6.43 ± 0.01	61.57 ± 0.02
TMV	6.11 ± 0.01	63.30 ± 0.06	6.13 ± 0.01	63.21 ± 0.01	6.13 ± 0.01	63.19 ± 0.02

Table 5. Day to Day Variation in Measured Mobility and Mobility Size

	first day		one week after		four weeks after	
	Z_p (10^{-8} m^{2}V^{-1}s^{-1})	D_p (nm)	Z_p (10^{-8} m^{2}V^{-1}s^{-1})	D_p (nm)	Z_p (10^{-8} m^{2}V^{-1}s^{-1})	D_p (nm)
BSA	467.52 ± 1.00	6.78 ± 0.01	466.84 ± 0.97	6.79 ± 0.01	468.91 ± 0.21	6.77 ± 0.02
IgG	259.12 ± 0.37	9.13 ± 0.01	258.09 ± 0.89	9.15 ± 0.02	257.38 ± 0.20	9.16 ± 0.01
PP7	37.28 ± 0.02	24.46 ± 0.01	36.99 ± 0.03	24.58 ± 0.01	37.23 ± 0.04	24.50 ± 0.01
PR772	6.41 ± 0.01	61.69 ± 0.04	6.42 ± 0.01	61.65 ± 0.01	6.40 ± 0.01	61.74 ± 0.15
TMV	6.04 ± 0.05	63.71 ± 0.06	6.11 ± 0.01	63.30 ± 0.06	6.10 ± 0.01	63.34 ± 0.02

the use of commercial nanoDMA (TSI), the same as we used here, caused the "anomalously large" mobility size,[6] they calibrated their DMA in a different way than we did: Maiβer et al. calibrated their DMA with [tetra-dodecyl ammonium]$^+$ ions, for which the mobility was measured by Ude and F. de la Mora,[7] while we used NIST traceable 100 nm size standard SRM1963. In addition, a different batch of BSA was studied here which could be a potential cause of difference. It remains unresolved whether the discrepancy in mobility arises from the different instrumental performance, the calibration method, variation of samples, or other factors.

CONCLUSION

In summary, we have measured the size distributions of several proteins and viruses: BSA, IgG, PP7, PR772, and TMV using ES-DMA and compared them with those of colloidal gold and PSL. The width of the size distribution of the bionanoparticles is a factor of at least two times smaller than that of the 30 and 60 nm PSL standards and a factor of about two times smaller than the gold nanoparticles. Transfer functions are calculated to show the instrument limits. The experimental results show the empirical spectra of bionanoparticles are less than 2.4 times wider than corresponding transfer functions where the worst case is PR772 with a ratio of 2.9 due to a possibility of temporal disintegration. By separating the contribution of diffusive transfer function, we also calculated the corrected distribution of the bionanoparticles, the width of which is 20% less than the empirical distribution. The fact that these corrected distributions are still wider than the transfer functions could result from multiple conformations of bionanoparticles due to capillary forces during the droplet evaporation process and from the presence of residual water or other volatile impurities. The nonideal behavior of the DMA is likely not a significant factor. Stability testing shows the mobility size of the bionanoparticles varies little as the buffer molarity or the buffer concentration changes. No significant change of mobility size is observed in the measurements for up to 4 weeks' time. Thus, the bionanoparticles could be a promising reference material for mobility size measurement.

AUTHOR INFORMATION

Corresponding Author
*E-mail: mrz@umd.edu.

Present Address
[†]S.G.: Food and Drug Administration, Silver Spring, MD.

Author Contributions
The manuscript was written through contributions of all authors. All authors have given approval to the final version of the manuscript.

Notes
The authors declare no competing financial interest.

REFERENCES

(1) Stefaniak, A. B.; Hackley, V. A.; Roebben, G.; Ehara, K.; Hamkin, S.; Postek, M. T.; Lynch, I.; Fu, W.; Linsinger, T. P. J.; Thünemann, F. *Nanotoxicology* **2013**, 7, 1325−1337.
(2) Guha, S.; Li, M.; Torlov, M. J.; Zachariah, M. R. *Trends Biotechnol.* **2012**, 30, 291−300.
(3) Knutson, E. O.; Whitby, K. T. *J. Aerosol Sci.* **1975**, 6, 443−451.
(4) Li, M.; You, R.; Mulholland, G. W.; Zachariah, M. R. *Aerosol Sci. Technol.* **2013**, 47, 1101−1107.
(5) Linsinger, T.; Roebben, G.; Solans, C.; Ramsch, R. *Trends Anal. Chem.* **2011**, 30, 18−27.
(6) Maiβer, A.; Premnath, V.; Ghosh, A.; Nguyen, T. A.; Attoui, M.; Hogan, C. J. *Phys. Chem. Chem. Phys.* **2011**, 13, 21630−21641.
(7) Ude, S.; de la Mora, J. F. *J. Aerosol Sci.* **2005**, 36, 1224−1237.
(8) Kaufman, S. L.; Skogen, J. W.; Dorman, F. D.; Zarrin, F. *Anal. Chem.* **1996**, 68, 1895−1904.
(9) Bacher, G.; Szymanski, W. W.; Kaufman, S. L.; Zollner, P.; Blaas, D.; Allmaier, G. *J. Mass Spectrom.* **2001**, 36, 1038−1058.
(10) Ku, B. K.; de la Mora, J. F. *Anal. Chem.* **2004**, 76, 814−822.
(11) Eninger, R. M.; Hogan, C. J.; Biswas, P.; Adhikari, A.; Reponen, T.; Grinshpun, S. A. *Aerosol Sci. Technol.* **2009**, 43, 298−304.
(12) Pease, L. F., III; Tsai, D.-H.; Brorson, K. A.; Guha, S.; Zachariah, M. R.; Tarlov, M. *J. Anal. Chem.* **2011**, 83, 1753−1759.

(13) Laschober, C.; Kaddis, C. S.; Reischl, G. P.; Loo, J. A.; Allmaier, G.; Szymanski, W. W. *J. Exp. Nanosci.* **2007**, *2*, 291−301.

(14) Tsai, D.-H.; Zangmeister, R. A.; Pease, L. F., III; Tarlov, M. J.; Zachariah, M. R. *Langmuir* **2008**, *24*, 8483−8490.

(15) Hinterwirth, H.; Wiedmer, S. K.; Moilanen, M.; Lehner, A.; Allmaier, G.; Waitz, T.; Lindner, W.; Lämmerhofer, M. *J. Sep. Sci.* **2013**, *36*, 2952−2961.

(16) Allen, M. D.; Raabe, O. G. *Aerosol Sci. Technol.* **1985**, *4*, 269−286.

(17) Guha, S.; Pease, L. F., III; Brorson, K. A.; Tarlov, M. J.; Zachariah, M. R. *J. Virol. Methods* **2011**, *178*, 201−208.

(18) Allmaier, G.; Laschober, C.; Szymanski, W. W. *J. Am. Soc. Mass. Spectrom.* **2008**, *19*, 1062−1068.

(19) Stolzenburg, M. R. An Ultrafine Aerosol Size Distibution Measuring System, Ph.D. Thesis, University of Minnesota Twin Cities, Minneapolis, 1988.

(20) Hagwood, C.; Sivathanu, Y.; Mulholland, G. *Aerosol Sci. Technol.* **1999**, *30*, 40−61.

(21) Attoui, M.; Paragano, M.; Cuevas, J.; de la Mora, J. F. *Aerosol Sci. Technol.* **2013**, *47*, 499−511.

(22) Hogan, C. J.; Ruotolo, B.; Robinson, C.; de la Mora, J. F. *J. Phys. Chem. B* **2011**, *115*, 3614−3621.

(23) Hogan, C. J.; Kettleson, E. M.; Ramaswami, B.; Chen, D.; Biswas, P. *Anal. Chem.* **2006**, *78*, 844−852.

(24) Banerjee, S.; Mazumdar, S. *Int. J. Anal. Chem.* **2012**, *2012*, 1−40.

6842

dx.doi.org/10.1021/ac403503q | *Anal. Chem.* 2014, 86, 6836−6842